

Direct synthesis of single-walled carbon nanotubes bridging metal electrodes by laser-assisted chemical vapor deposition

J. Shi, Y. F. Lu,^{a)} and K. J. Yi

Department of Electrical Engineering, University of Nebraska—Lincoln, Lincoln, Nebraska 68588-0511

Y. S. Lin and S. H. Liou

Department of Physics and Astronomy, University of Nebraska—Lincoln, Lincoln, Nebraska 68588-0111

J. B. Hou and X. W. Wang

Department of Mechanical Engineering, University of Nebraska—Lincoln, Lincoln, Nebraska 68588-0656

(Received 7 April 2006; accepted 17 July 2006; published online 21 August 2006)

Direct synthesis of single-walled carbon nanotubes (SWNTs) bridging prepatterned Mo electrodes has been achieved using laser-assisted chemical vapor deposition (LCVD). The synthesized SWNTs are found predominantly semiconducting. By controlling the spot size of the focused laser beam, synthesis of SWNTs can be achieved in a localized manner, which is governed by the thermal and optical properties of materials as well as the laser parameters. The synthesis process is fast and can be achieved in both far- and near-infrared laser wavelength regions. LCVD method provides a potential approach to *in situ* remove SWNTs with specific chiralities during the growth. © 2006 American Institute of Physics. [DOI: 10.1063/1.2338005]

Since the demonstration of the room-temperature carbon nanotube (CNT) field effect transistor,¹ intensive studies have been carried out in the improvement of CNT-device fabrication processes^{2,3} and device performances.^{4–6} From the early postgrowth assembly method^{1,7} to the electrical-field-directed thermal chemical vapor deposition (CVD) technique,^{8,9} there have been significant advances in the control of position and orientation in CNT synthesis.

Among various CNT synthesis methods, laser-assisted chemical vapor deposition (LCVD) is a promising alternative that has emerged recently.^{10–14} LCVD technique, in general, uses laser to locally create a hot spot on the substrate surfaces. CVD occurs at the gas-substrate interface when the reactant molecules are catalytically pyrolyzed at the catalysts within or in the vicinity of the hot spot, leading to the subsequent formation of CNTs. LCVD process has several unique features over other conventional CVD techniques. First, LCVD is inherently a cold-wall process, in which laser can be focused on a preferred location to induce local heating instead of overall chamber/substrate heating which is common in conventional CVD techniques.¹² Second, it is a fast heating process (laser can instantly heat the substrate to a desired high temperature), which is particularly beneficial to the growth of long and well-aligned single-walled carbon nanotubes (SWNTs).¹⁵ Third, by expanding or focusing the laser beam, the process can be switched between large-area and local modes. Most importantly, due to the resonant absorptions of SWNTs at specific Van Hove singularities,¹⁶ lasers can potentially affect the chiralities of SWNTs during the growth process when the wavelength of the incident laser matches the resonant absorption wavelength of the SWNTs. Recent results for SWNT chirality selection by laser resonant oxidation¹⁷ justified such feasibility. Utilizing both thermal and optical effects, the LCVD technique, thus, provides the

possibility to combine SWNT growth and chirality selection in a single process.

In this study, we demonstrated position-controlled synthesis of SWNTs which can bridge the predefined electrodes using the LCVD technique. The synthesized SWNTs showed predominantly semiconducting characteristics. The synthesis process is very fast and can be conducted in both far- and near-infrared wavelength regions. By controlling the focused laser beam size, SWNTs can be synthesized in a localized manner.

Figure 1 shows the schematic diagram of the electrical-field-directed LCVD system. Heavily doped *p*-type silicon substrates with a 2- μm -thick thermal oxide were used in the experiments. Mo electrodes were fabricated by first depositing a 100-nm-thick Mo films on patterned photoresist on substrates using dc sputtering, followed by a lift-off process. Due to its high melting point (2625 °C), Mo is suitable for the process having localized high temperature under focused laser irradiation. The catalyst used for SWNT growth was Fe–Mo–alumina porous structures¹⁸ [a mixture of

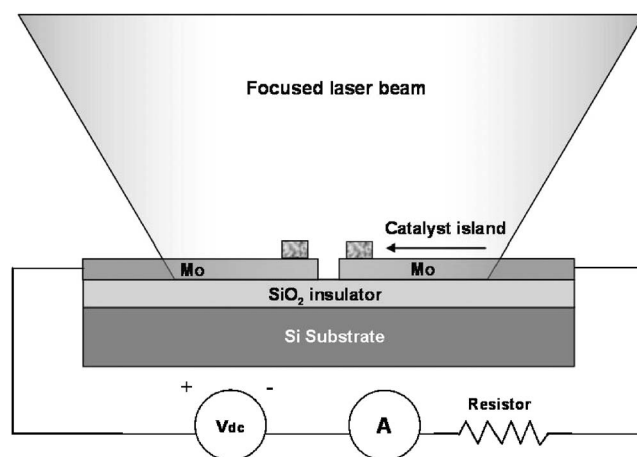


FIG. 1. Schematic diagram of electrical-field-directed laser-assisted CVD system.

^{a)} Author to whom correspondence should be addressed; electronic mail: ylu2@unl.edu

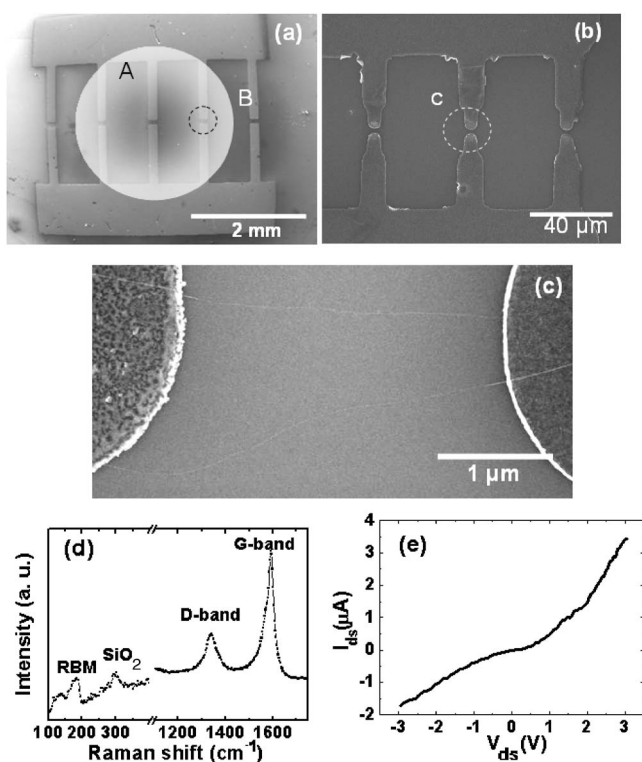


FIG. 2. (a) SEM micrograph of patterned Mo electrodes. Circle “A” is the typical unfocused 2 mm CO₂ laser beam irradiated on the substrate, while circle “B” is the typical focused laser beam with beam size of 340 μm using a 10 cm ZnSe lens. (b) Magnified electrode pairs inside circle B shown in (a). (c) SEM micrograph of two SWNTs bridging the electrodes inside circle “C” shown in (b). (d) Raman spectroscopy of SWNTs shown in (c). (e) I-V curve of the SWNTs shown in (c).

Fe(NO₃)₃·9H₂O, MoO₂(acac)₂, and alumina nanopowder in de-ionized water]. Shipley 1813 was used as the photoresist in patterning of both catalyst islands and electrodes. The LCVD process was conducted in a vacuum chamber. A continuous wave (cw) CO₂ laser (Synrad, firestar v40, wavelength of 10.6 μm) or a cw Nd:YAG (yttrium aluminum garnet) laser (Quantronix Inc., condor 200M, wavelength of 1064 nm) was used to irradiate the substrate respectively. A dc power supply and an ampere meter were connected in the circuit, as shown in Fig. 1. In the experiments, a dc bias was applied across the electrodes to introduce a directing electrical field for aligned growth of SWNTs.⁸ The magnitude of the dc bias varied according to the gap width, with typical values of 1–1.5 V/μm. The ampere meter was used to detect the current flow in the circuit when SWNTs bridged electrodes, which enabled *in situ* monitoring of the growth condition and detection of the end point of the process. A 10 kΩ resistor was connected in the circuit to protect SWNTs from being burnt due to a large short current. Before the CVD process, the vacuum chamber was first pumped down to 1 × 10⁻³ Torr. Acetylene and ammonia (C₂H₂/NH₃) gas mixture with a volume ratio of 1/10 were then introduced into the chamber. The gas pressure was stabilized during the process with a process window between 1 and 100 Torr. During the laser irradiation, a pyrometer (Omega, single color OS 3750) was used to monitor the substrate temperature at the laser spot. The reaction temperature was controlled in a range from 690 to 720 °C. The growth period varied from 3 to 6 min.

Figure 2(a) shows the scanning electron microscope

(SEM) micrograph of the patterned Mo electrodes. Circle “A” indicates a typical unfocused 2 mm CO₂ laser beam irradiated on the substrate. Circle “B” indicates a typical focused laser spot (340 μm) using a ZnSe lens (focal length of 10 cm), which covers a single bar. An enlarged view of circle B is shown in Fig. 2(b). Usually, three to four pairs of parallel electrodes were fabricated with gap widths varied from 1 to 4 μm depending on the lithography. After the growth, each pair was isolated for individual measurement of electrical transfer characteristics. Figure 2(c) shows a typical SEM micrograph of two long SWNTs bridging the electrodes under an unfocused laser beam. Typical CO₂ laser power was about 20–25 W, corresponding to a power density of 6.4–8.0 MW/m². During the process, the region under the laser beam turned red and reached the desired temperature almost immediately after the laser started irradiation. Sharp temperature gradient on the sample was observed, indicating that a localized heating was achieved. The temperature of the sample stage remained at about 200 °C during the laser irradiation. We observed that such bridging process typically took only about 20–30 s, after which the current started to flow in the circuit on an order of several microamperes. SWNTs could sustain continuous laser irradiation without getting burnt after bridging the electrodes. However, when we intentionally increased the laser power, particularly when the beam center temperature was above 1000 °C, current flowing in the circuit quickly dropped to zero. SEM micrographs confirmed the discontinuity of long SWNT at the edges of the electrodes. At a proper laser power density, Mo electrodes were free of damage. When the laser power density was increased, the electrode surface became roughened and the resistance of the electrodes increased by two orders of magnitude. Figure 2(d) shows the Raman spectrum of the SWNTs which were shown in Fig. 2(c). The sample was excited by an argon ion laser at 514.5 nm. At the high frequency region, a sharp G band at around 1591 cm⁻¹ is observed. The presence of a D band at 1350 cm⁻¹ indicates that there might be some amorphous carbon synthesized. In the low frequency region, the feature at about 300 cm⁻¹ is attributed to SiO₂.¹⁹ The peak at about 178 cm⁻¹ is attributed to the characteristic radial breathing mode (RBM) of the SWNTs. By applying the relationship between the SWNT diameter *d* (nm) and Raman shift λ (cm⁻¹), $d=248/\lambda$,²⁰ the average diameter of the SWNTs is estimated to be 1.4 nm. Figure 2(e) shows the I-V curve of the SWNTs shown in Fig. 2(c). A voltage bias scanning from -3 to 3 V was added between two electrodes of the structure, as shown in Fig. 1. The gap-related nonlinearity indicates that the SWNTs are semiconducting. From the I-V characteristics, so far, all the SWNTs synthesized using CO₂ laser based LCVD system are found to be semiconducting. Further investigations are needed to reveal the mechanisms behind the preferred synthesis of semiconducting SWNTs.

By focusing the laser beam, local synthesis of SWNTs which bridged two electrodes was also achieved. In this case, the applied laser power was 12 W with a focused spot size of about 340 μm achieved using a ZnSe lens (focal length of 10 cm). The focused beam covered one of the five vertical bars, with the area approximately same as circle B shown in Fig. 2(a). Figure 3 shows the SEM micrograph of SWNTs bridging a pair of electrode under a focused CO₂ laser beam. The arrow shown in Fig. 3 indicated two blurred lines which were suggested to be part of the SWNTs lying on the sub-

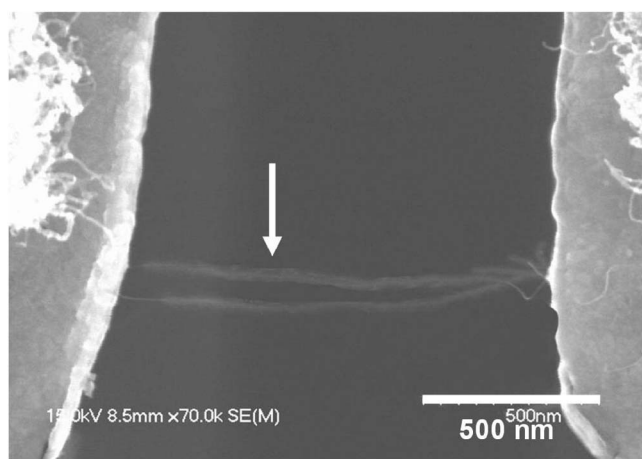


FIG. 3. SEM micrograph of two SWNTs bridging the electrodes synthesized by a focused CO₂ laser beam with a beam size of 340 μm in diameter.

strate. The height difference between the substrate and electrodes resulted in the lack of focus in the SEM micrograph of those SWNTs. SWNTs were observed only in the area under the focused laser beam, where other electrodes with the same catalyst islands remained intact. Note that it is possible to push the localization to a few microns in diameter by selecting lasers with shorter wavelengths, lens with high numeric aperture, and appropriate laser power densities.¹²

We have also grown SWNTs using a near-infrared Nd:YAG laser at 1064 nm. The typical laser power was 60 W, with a beam size of 6 mm in diameter. Individual SWNTs grew radially out of the catalyst island. The corresponding Raman spectrum has a characteristic RBM peak at 204 cm⁻¹. The average diameter of SWNTs is estimated to be about 1.2 nm.

In summary, we have demonstrated synthesis of SWNTs over predefined electrodes using the LCVD technique. The synthesis can be conducted using both far-infrared CO₂ laser (10.6 μm) and near-infrared Nd:YAG laser (1064 nm). We have also demonstrated localized synthesis of SWNTs by a focused laser beam. Due to the unique advantages of LCVD process, such as fast and local heating, as well as its potential

to select chiralities during the grow, it may provide additional features and versatility in the device fabrication.

The authors would like to express their appreciation to the National Science Foundation grants (DMI 0444027 and DMI 0555884), the NSF MRSEC at the University of Nebraska-Lincoln, and the Nebraska Research Initiative for supporting this research work.

- ¹S. J. Tans, A. R. M. Verschueren, and C. Dekker, *Nature (London)* **393**, 49 (1998).
- ²G. Zhang, D. Mann, L. Zhang, A. Javey, Y. Li, E. Yenilmez, Q. Wang, J. P. McVittie, Y. Nishi, J. Gibbons, and H. Dai, *Proc. Natl. Acad. Sci. U.S.A.* **102**, 16141 (2005).
- ³K. Hata, D. N. Futaba, K. Mizuno, T. Namai, M. Yumura, and S. Iijima, *Science* **306**, 1362 (2004).
- ⁴V. Derycke, R. Martel, J. Appenzeller, and Ph. Avouris, *Appl. Phys. Lett.* **80**, 2273 (2005).
- ⁵A. Javey, H. Kim, M. Brink, Q. Wang, A. Ural, J. Guo, P. McIntyre, P. McEuen, M. Lundstrom, and H. Dai, *Nat. Mater.* **1**, 241 (2002).
- ⁶Y. Noshu, Y. Ohno, S. Kishimoto, and T. Mizutani, *Appl. Phys. Lett.* **86**, 073105 (2005).
- ⁷R. Martel, T. Schmidt, H. R. Shea, T. Hertel, and Ph. Avouris, *Appl. Phys. Lett.* **73**, 2447 (1998).
- ⁸A. Ural, Y. M. Li, and H. J. Dai, *Appl. Phys. Lett.* **81**, 3464 (2002).
- ⁹Y. G. Zhang, A. L. Chang, and H. J. Dai, *Appl. Phys. Lett.* **79**, 3155 (2001).
- ¹⁰Y. Fujiwara, K. Maehashi, Y. Ohno, K. Inoue, and K. Matsumoto, *Jpn. J. Appl. Phys., Part 1* **44**, 1581 (2005).
- ¹¹K. Kwok and W. K. S. Chiu, *Carbon* **43**, 437 (2005).
- ¹²F. Rohmund, R.-E. Morjan, G. Ledoux, F. Huisken, and R. Alexandrescu, *J. Vac. Sci. Technol. B* **20**, 802 (2002).
- ¹³S. N. Bondi, W. J. Lackey, R. W. Johnson, X. Wang, and Z. L. Wang, *Carbon* **44**, 1393 (2006).
- ¹⁴K. Kwok and W. K. S. Chiu, *Carbon* **43**, 2571 (2005).
- ¹⁵S. Huang, X. Cai, and J. Liu, *J. Am. Chem. Soc.* **125**, 563 (2003).
- ¹⁶H. Kataura, Y. Kumazawa, I. Umezu, S. Suzuki, Y. Ohtsuka, and Y. Achiba, *Synth. Met.* **103**, 2555 (1999).
- ¹⁷K. Maehashi, Y. Ohno, K. Inoue, and K. Matsumoto, *Appl. Phys. Lett.* **85**, 858 (2004).
- ¹⁸J. Kong, H. T. Soh, A. Cassell, C. F. Quate, and H. Dai, *Nature (London)* **395**, 878 (1998).
- ¹⁹M. S. Dresselhaus, G. Dresselhaus, R. Saito, and A. Jorio, *Phys. Rep.* **409**, 47 (2005).
- ²⁰A. Jorio, R. Saito, J. H. Hafner, C. M. Lieber, M. Hunter, T. McClure, G. Dresselhaus, and M. S. Dresselhaus, *Phys. Rev. Lett.* **86**, 1118 (2001).